El Niño–Southern Oscillation and the Transatlantic Slave Trade

WILLIAM TURNER IV[a] AND TERRENCE R. NATHAN[a]

[a] *Atmospheric Science Program, Department of Land, Air, and Water Resources, University of California, Davis, Davis, California*

ABSTRACT: The relationship between El Niño–Southern Oscillation (ENSO) and the transatlantic slave trade (TAST) is examined using the Slave Voyages dataset and several reconstructed ENSO indices. The ENSO indices are used as a proxy for West African rainfall and temperature. In the Sahel, the El Niño (warm) phase of ENSO is associated with less rainfall and warmer temperatures, whereas the La Niña (cold) phase of ENSO is associated with more rainfall and cooler temperatures. The association between ENSO and the TAST is weak but statistically significant at a 2-yr lag. In this case, El Niño (drier and warmer) years are associated with a decrease in the export of enslaved Africans. The response of the TAST to El Niño is explained in terms of the societal response to agricultural stresses brought on by less rainfall and warmer temperatures. ENSO-induced changes to the TAST are briefly discussed in light of climate-induced movements of peoples in centuries past and the drought-induced movement of peoples in the Middle East today.

SIGNIFICANCE STATEMENT: The transatlantic slave trade was driven by economic and political forces, subject to the vagaries of the weather; it spanned two hemispheres and four continents and lasted more than 400 years. In this study we show that El Niño–Southern Oscillation, and its proxy association with West African rainfall and temperature, are significantly associated with the number of enslaved Africans that were transported from West Africa to the Americas. Lessons learned from the effects of weather and climate on the transatlantic slave trade reverberate today: extreme weather and climate change will continue to catalyze and amplify human conflict and migrations.

KEYWORDS: Africa; Drought; Climate change; El Niño; History

1. Introduction

From 1440 to 1870, economic forces produced the largest forced migration in history: The transatlantic slave trade (TAST). More than 12 million enslaved Africans were forcibly placed in shackles and loaded on ships bound for the Americas.[1] The transatlantic voyages lasted several months. Of the enslaved Africans that survived the voyage, approximately 36% arrived in the British, French, Dutch, and Danish West Indies; 35% arrived in Brazil; 22% arrived in Latin America and the Caribbean Sea region; 5% arrived in the United States; and 2% arrived in Europe (Thomas 1997).

The TAST was characterized by pronounced variability in the number of slaves exported from Africa to the Americas. The variability was a consequence of economic forces (Eltis 1987a,b), political upheavals (Thomas 1997; M'baye 2006), and extreme weather events (Miller 1982; Fenske and Kala 2015).

The economic forces that operated on the TAST were driven by the global appetite for commodities such as sugar, tobacco, and cotton (Craton 1974). To meet the global demand and the ever-growing zeal for profit required cheap labor. The demand for sugar, for example, increased the demand for enslaved Africans in Caribbean islands such as the West Indies (Craton 1974; Eltis et al. 2005). The global demand for tobacco increased the demand for enslaved Africans throughout Brazil, Cuba, and the southern United States (Eltis 1987b). After the invention of the cotton gin in 1793, cotton production became profitable, which accelerated the need for slave labor throughout the southern United States (Bailey 1994). The profits generated on the backs of the enslaved Africans were then used to fuel the Industrial Revolution (Craton 1974; Mintz 1986; Bailey 1994).

Political upheavals erupted throughout the TAST (Table 1). Wars, revolutions, and changes in laws governing the slave trade each affected the TAST. The Seven Years' War, for example, which spanned 1756–63, began as a battle for territorial control by the British, French, and Spanish Empires (Anderson 2000). After Britain won the war, the number of slaves in their American territories increased. Unlike the Seven Years' War, the American Revolution (1765–83) and the Haitian Revolution (1791–1804) each led to a decrease in the number of slaves exported to the Americas (Du Bois 1896; Blackburn 1988). The decrease was associated, in part, with an increase in the costs for slaves during the American Revolution (Du Bois 1896) and with a successful Haitian revolt against the French who controlled one-half of the Caribbean island of Hispaniola (Blackburn 1988).

---

[1] Here we use the words *enslaved* and *slave* interchangeably, although recently there has been an evolution toward the more humanizing phrase, *enslaved individuals*. The largest slave ships carried as many as 700 enslaved Africans, with ~3 ft^2 (0.3 m^2) allotted to each individual (Rediker 2007).

Denotes content that is immediately available upon publication as open access.

Corresponding author: William Turner IV, wturneriv@ucdavis.edu

TABLE 1. Major political events and wars during the TAST.

Event	Dates
War of the Austrian Succession	1740–48
Seven Years' War	1756–63
American Revolution	1765–83
Haitian Revolution	1791–1804
Abolition of the Slave Trade Act	1807
Anglo-Brazilian Anti-Slave Trade Treaty	1830

From the late 1700s to the early 1800s, Britain experienced political tumult that sprung from the proposed abolition of the TAST. This led to an attempt to abolish the slave trade when Britain enacted the Slave Trade Act in 1807, which prohibited the slave trade throughout the British Empire (Anstey 1972). Decades would pass, however, before the British enacted the Slavery Abolition Act in 1833, which formalized Britain's departure from the TAST.

After Brazil declared independence from Portugal, Brazil attempted to end the slave trade through the Anglo-Brazilian Anti-Slave Trade Treaty of 1827 (Bethell 1966). Yet, it was not until 1850, a span of 23 years, that the Brazilian slave trade would formally be abolished (Needell 2001).

The economic forces and political upheavals that occurred during the TAST were subject to the vagaries of the weather (Mulcahy 2004). For example, Saharan dust storms often swept across North Africa, which were documented by ships near the slave-trading ports located along the West African coast (NCDC 1998). The dust storms have been shown to affect the development and movement of hurricanes in the eastern Atlantic Ocean (Chen et al. 2015). Once formed, the hurricanes moved westward, eventually reaching landfall where they destroyed ships, ports, towns, and agricultural storage facilities that provided the infrastructure needed to fuel the economic engine that drove the TAST (Sheridan 1976; Mulcahy 2004). The effects of hurricanes often extended beyond damage to infrastructure and agriculture; they resulted in extensive casualties, particularly among the slave population in the Caribbean. The Great Hurricane of 1780, for example, killed approximately 2000 Barbadian slaves and reduced the export of sugar, rice, and rum, which had a deleterious effect on the British slave economy (Sheridan 1976; Mulcahy 2004).

Like the Caribbean, West Africa experienced extreme weather events that influenced the TAST. Among the most common events were droughts, which exacerbated economic hardships and sparked internal conflicts (Miller 1982).

Formally, drought can be defined as "a period of abnormally dry weather sufficiently long enough to cause a serious hydrological imbalance . . . Drought is a relative term, therefore any discussion in terms of precipitation deficit must refer to the particular precipitation-related activity that is under discussion" (American Meteorological Society 2020). Because there are different types of precipitation-related events, there are several types of droughts. For example, the National Centers for Environmental Information define four types of droughts: 1) meteorological, 2) hydrological, 3) agricultural, and 4) socioeconomic. Meteorological drought occurs when

dry weather patterns, or rainfall deficits, dominate an area for a sufficiently long period. Hydrological drought occurs after many months of meteorological drought, when low water supply becomes evident in rivers, lakes, groundwater, and reservoirs. Agricultural drought occurs when crops become affected by water resource deficits. And socioeconomic drought relates the impact of drought conditions on the supply and demand of various commodities, such as fruits, vegetables, and meat (NCEI 2020).

Historians have asserted that drought-induced stresses on West African (WA) societies increased the number of enslaved Africans exported to the Americas (Dias 1981; Miller 1982; Lovejoy 2012). Their assertions were based on qualitative descriptions of weather events written in historical documents such as memoirs, journals, chronicles, and national archives. Lovejoy and Baier (1975), for example, identified droughts from several sources including the "Kano Chronicle," which is a written history of Hausa people in Nigeria dating back to the tenth century. This chronicle, among others, referenced agricultural productivity, famines, and lake-level variations. Miller (1982) cited short-term weather events from Portuguese observations and long-term weather events from African oral traditions. Some events that were associated with severe droughts have been associated with changes in the number of enslaved Africans (Dias 1981; Miller 1982; Lovejoy 2012). Dias (1981), for example, states, "In October 1857, following two years of drought and crop failure, men and women from Kisama inundated local markets on the north bank of the Kwanza, exchanging their own, or their relatives', freedom for small bags containing a mixture of manioc flour, beans, maize and groundnuts. Demand for slaves was very high." Miller (1982), who extended the work of Dias (1981), stated, "The historic peaks in the exports [of enslaved Africans] from both Luanda and Benguela in the 1790s came as the most severe drought of the entire century ran its course." Lovejoy (2012, p. 70) states, "Many people, not just slaves, found themselves in a desperate condition, as traditions from the Senegal River valley demonstrate for the middle of the eighteenth century, when the number of slaves apparently increased as a result of this suffering."

Economists Fenske and Kala (2015) took a different approach from that of the historians. Rather than examine qualitatively how droughts affected the TAST, they examined statistically how anomalous temperatures affected the TAST. Their approach relied on the notion of shocks, an approach commonly used in economics to examine how an unexpected event affects an economy. In their study, Fenske and Kala (2015) examined how "environmental shocks shaped the dynamics of the transatlantic slave trade." To do so they used a Tobit model, a type of regression model, to correlate the Mann et al. (1998) reconstructed global temperatures, which date back to the fifteenth century, with the number of enslaved Africans transported from African slave-trading ports to the Americas. Their analysis hinged on interpolating the gridded temperature data to 134 African slave-trading ports, which they correlated with the number of slaves exported from African ports between 1730 and 1866. They found a significant correlation between anomalously warm

temperatures and a decrease in the number of African slaves transported to the Americas. The correlation was at a zero lag, meaning the anomalous temperatures produced a response in the TAST during the same year.[2] Fenske and Kala (2015) suggested that the reduction in slave exports was due to increased agricultural stresses brought on by the warmer temperatures. They argued that the warmer temperatures produced "environmental shocks" that "raised the costs of slaving," which manifested in an overall reduction in the number of enslaved Africans exported to the Americas. Fenske and Kala's (2015) analysis, however, did not address the cause of the temperature anomalies.

More recently, Boxell (2019) examined how both temperature and rainfall influenced the TAST. He focused on the period 1801–66, a period that spans ~15% of the lifetime of the TAST. This relatively short period was chosen because proxy and instrumental rainfall data are both available for most of the African slave-trading regions. Like Fenske and Kala (2015), Boxell (2019) approached the study from the perspective of environmental shocks, in which he used a Tobit model to calculate the correlations. For the temperature–TAST correlation, Boxell (2019) used Mann et al.'s (1998) reconstructed temperatures; for the rainfall–TAST correlation, he used Nicholson's (2001) African rainfall data. Boxell (2019) found 1) warmer and cooler temperatures are significantly correlated with an increase in the number of enslaved Africans transported to the Americas, and 2) a decrease in rainfall is significantly correlated with an increase in the number of enslaved Africans transported to the Americas. Boxell (2019) suggested that the decreases in rainfall exacerbated interethnic group conflict, which resulted in the increase in slave exports. However, Boxell (2019), like Fenske and Kala (2015), did not address the cause of the temperature or rainfall anomalies.

Here we opt for a different but complementary approach to that of Fenske and Kala (2015) and Boxell (2019). Rather than use rainfall and temperature data, which are temporally and spatially limited over Africa for the period and region to be considered here, we use an El Niño–Southern Oscillation (ENSO) index as a proxy for anomalous WA rainfall and temperature. Doing so not only allows us to cover a longer portion of the TAST, it also provides a physical mechanism for the precipitation and temperature anomalies. In our analysis, we examine ENSO-induced anomalies in both rainfall and temperature, although we focus on the former, since rainfall outweighs temperature when it comes to agricultural production (Nieuwolt 1982; Lobell and Burke 2008).
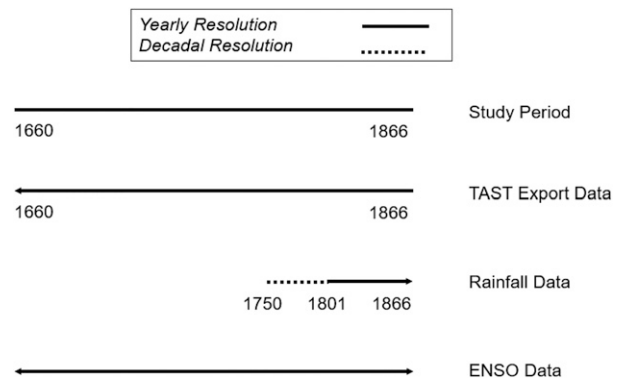

FIG. 1. The period of this study is 1660–1866. The data available for this period include TAST export data (Eltis et al. 2009) from 1501 to 1866, annual rainfall data (Nicholson et al. 2012) from 1801 to 1998, decadal-resolution rainfall data (Norrgård 2015) from 1750 to 1800, and annual rainfall data (Mitchell 2016) from 1900 to 2016. The reconstructed ENSO data are based on several sources: Quinn et al. (1987) (1525–1987), Cook et al. (2008) (1300–1929), Gergis and Fowler (2009) (1525–2002), and McGregor et al. (2010) (1650–1977). See the text for additional details.

Our study is framed by the following hypothesis: ENSO and its relationship to WA rainfall and temperature modulated the number of enslaved Africans that were transported from West Africa to the Americas. To test our hypothesis, we use the Trans-Atlantic Slave Trade database and a reconstructed ENSO index, which we use as a proxy for WA rainfall and temperature. We then show that there is a small but statistically significant association between ENSO-induced rainfall and temperature anomalies and the TAST.

The paper is organized as follows: section 2 describes the data and research methods used to determine the correlations between ENSO and the TAST. Section 3 presents the results and their interpretation, and section 4 presents the conclusions, opportunities for further study, and how lessons learned from ENSO-induced changes to the TAST can inform how societies have responded to climate-induced changes in the movement of peoples in the past and today.

2. Data and methods

In this section we discuss (i) the region for the analysis, (ii) the TAST database, (iii) the period for the analysis, (iv) the statistical method, (v) ENSO as a proxy for WA rainfall, and (vi) the selection of reconstructed ENSO indices. The data used in this study and the periods over which they are available are summarized in Fig. 1 and discussed below.

a. Analysis region

Our analysis focuses on West Africa, a region we define as 5°–20°N and 20°W–15°E (Fig. 2). Based on the Köppen climate classification system, this region includes two climate zones: 1) A semiarid region: the Sahel; and 2) a tropical region: the West African coast. Along the coast, major slave-trading ports were in Senegambia and offshore Atlantic

---

[2] We have confirmed Fenske and Kala's (2015) results. As in their study, we used a Tobit model to relate the Mann et al. (1998) reconstructed temperatures with the TAST for the period spanning 1730–1866. In contrast to their analysis, however, in which they used slave export data from select African ports, we used slave export data for the whole West African region. Despite the different datasets, we find, in agreement with Fenske and Kala (2015), that an increase in temperatures is significantly associated with a decrease in the number of enslaved Africans exported to the Americas.
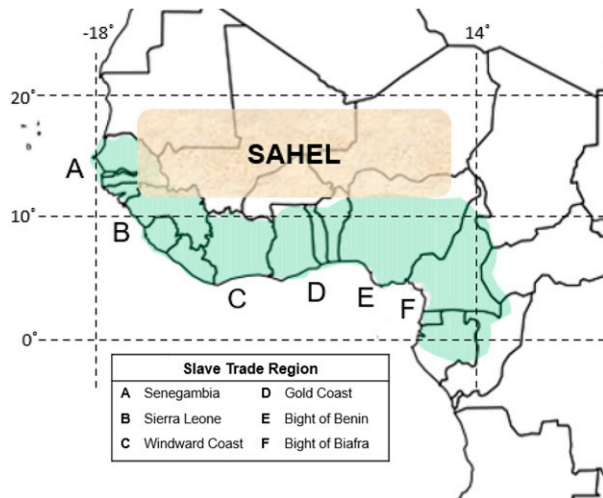
FIG. 2. Present-day political boundaries in West Africa overlaid with the approximate location of the West African Sahel (tan shading) and the West African slave-trading regions (green shading).

(currently Senegal, Gambia, and Cape Verde); Sierra Leone; the Windward Coast (currently Ivory Coast and Liberia); the Gold Coast (currently Ghana); the Bight of Benin (currently Togo and Benin); and the Bight of Biafra (currently Gabon) (Curtin 1972).

b. TAST database

The Trans-Atlantic Slave Trade database (Eltis et al. 2009), also known as the Slave Voyages database, includes the annual number of enslaved Africans that embarked in West Africa from 1501 to 1866 (Fig. 3a). The data were derived from historical archives, including personal journals and diaries, ship logs, newspapers, and chronicles. Only 18 years, about 5% of all the years available, are missing data, where most of the missing data occur before 1650. To fill the data gaps, we linearly interpolated the data by taking the mean of the estimates from the preceding and succeeding years surrounding the gap. After interpolation, the total estimate of enslaved West Africans transported from Africa to the Americas from 1501 to 1866 was 6 313 789. The maximum occurred in 1770, when ~68 000 enslaved West Africans were transported out of West Africa. The annual number of enslaved West Africans was relatively small and steady until about 1650, after which the numbers rapidly grew, reached its zenith in the mid-1700s, and then rapidly declined until the demise of the TAST in the mid-1800s.

c. Analysis period

The growth and decline of the TAST is evident in the z scores shown in Fig. 3b, which measure how many standard deviations the annual export of West African slaves is from the 1501 to 1866 mean. The z score is calculated as the difference between the annual number and the mean of enslaved West Africans, and then normalized by the standard deviation; z scores greater than $+1$ or less than -1 represent anomalous high or low exports, respectively. The z scores indicate that the TAST was most active between 1700 and 1800. For this period,

the total number of exported slaves was 4 093 867 and averaged 40 533 yr^{-1} with a standard deviation of 13 213 yr^{-1}. The period 1700–1800 represents ~65% of the total number of exported West African slaves, while the average for this period is more than double that of the period spanning 1501–1866.

Here we focus on the period 1660–1866, which includes the time when the TAST grew most rapidly and when it eventually ended. This period contains ~95% (5 983 365) of the total number of enslaved West Africans during 1501–1866, an average of 28 905 yr^{-1} with a standard deviation of 17 272 yr^{-1}.

d. Statistical method

To prepare the data for statistical analysis, we first obtain the power spectrum (Fig. 4) for the annual number of enslaved Africans transported from West Africa to the Americas between 1660 and 1866. Figure 4 shows that the largest frequencies fall within the 10–25-yr range. This suggests that over these frequency bands there were major events that affected the TAST. For example, as shown in Table 1, there were major political events and wars that took place during the TAST. The difference between the start date of the wars and political events ranged between 9 and 26 years, which falls within the 10–25-yr frequency band.

To ensure the data are not overly influenced by the dominant frequencies, whose time scales are outside of our interest, we detrend the data. Before doing so, however, we take the natural logarithm of the TAST data and then use a high-pass filter to remove the centered moving average of 8 years. This isolates the shorter, interannual trends, which are more apt to be associated with extreme weather events, including droughts and floods. The detrended data were then normalized by the standard deviation, which yields the time series used for the statistical analyses presented in sections 2e and 2f.

Figure 5 shows the raw data (left column) and the detrended data (right column) for three groupings: the TAST data for the period 1660–1866, an example of a reconstructed ENSO index used in this study (McGregor et al. 2010), and a scatterplot that provides a visual "first guess" of the relationship between ENSO and the TAST at a 2-yr lag. Not surprisingly, the scatterplot based on the raw data shown in Fig. 5c shows little or no correlation, a consequence of the many interrelated and complex forces that operated on the TAST, which include socioeconomic, political, and environmental forces. However, a correlation between ENSO and the TAST at the 2-yr lag is visually evident in the scatterplot shown in Fig. 5f, which is based on the detrended data. The correlation, which appears to have a negative slope, will be shown in section 3 to be the most statistically significant.

Our statistical analysis shows that the TAST and ENSO data are each autocorrelated, which can overstate the relationship between the two. To reduce the autocorrelation that exists for each dataset, we use the Newey–West heteroskedasticity and autocorrelation consistent covariance matrix (Newey and West 1987). After application of the
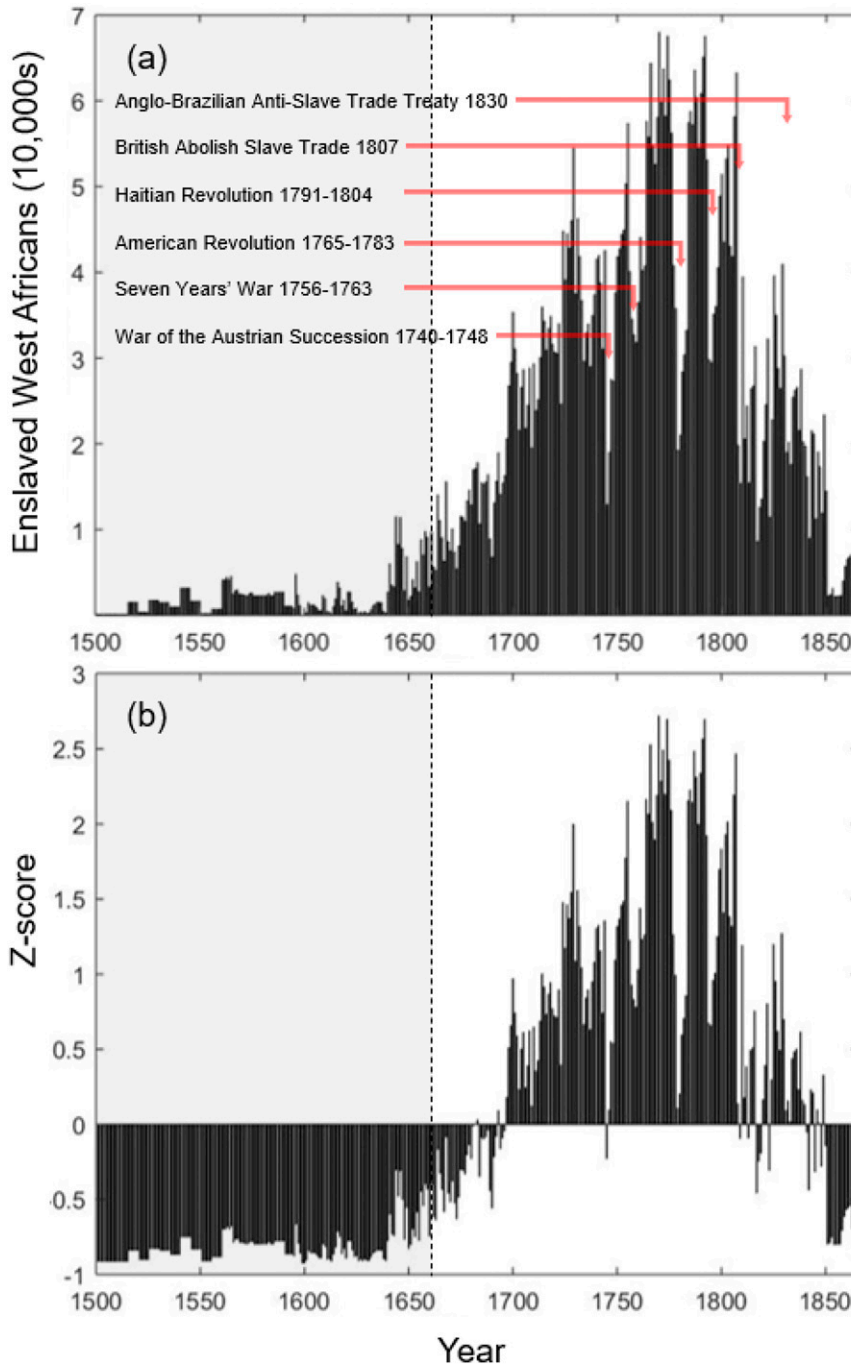
FIG. 3. (a) Annual number of enslaved West Africans transported from West Africa to the Americas from 1501 to 1866. Data are from the Slave Voyages database (http://www.slavevoyages.org; Eltis et al. 2009). The shaded region denotes annual enslaved exports prior to our study period of 1660–1866. Major political events and wars listed in Table 1 are also shown with their corresponding dates. (b) The z scores of the number of enslaved West Africans transported to the Americas. Anomalously large transports occur between 1700 and 1800.

Newey–West method, we use a multivariate regression analysis, one that depends on four lagged ENSO predictor variables, which span 0–3 years. The multiple linear regression model identifies the lags that are most important.

To assess the statistical significance of the coefficients obtained from the multiple linear regression model, we follow standard practice and use the p value (Wilks 2006). Traditionally, $p = 0.05$ is used as a cutoff; p values less
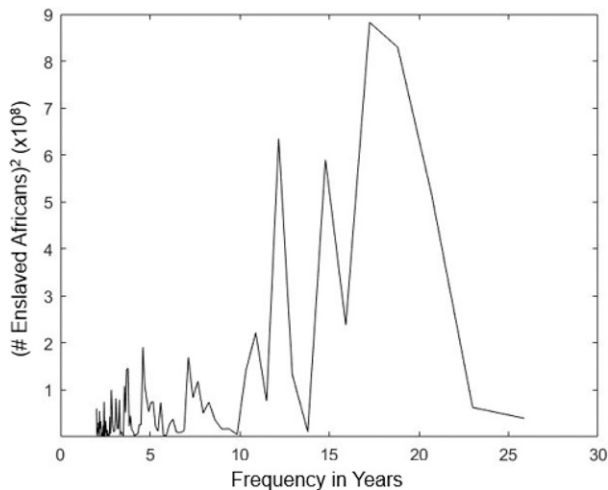
FIG. 4. Power spectrum for the annual number of enslaved West Africans transported to the Americas from 1660 to 1866. The dominant frequency bands fall within the 10–25-yr range, which contain the global political events and wars listed in Table 1.

than 0.05 are deemed statistically significant. But, as discussed by Amrhein et al. (2019a,b), Wasserstein et al. (2019) and others, p values above 0.05 do not necessarily mean that the correlations are insignificant. As Amrhein et al. (2019a) make clear, when making statistical inferences, "understanding of underlying mechanisms [is] often more important than statistical measures such as P values." This view is shared by McShane et al. (2019), who suggest that p values "be considered along with currently subordinate factors (e.g., related prior evidence, plausibility of mechanism, study design and data quality . . .) as just one of many pieces of evidence." With these caveats in mind, we note $p < 0.05$ for several of the statistical associations that we present later.

e. ENSO as a proxy for West African rainfall

1) DATA AVAILABILITY

Instrumental rain gauge data for West Africa during the TAST is scant. To reconstruct past weather and climate over the region, the limited instrumental data must be supplemented with proxy data, such as tree rings, lake sediments, pollen samples, and descriptive documentary data. Nicholson et al. (2012), for example, used a combination of instrumental rain gauge and proxy data to develop annual rainfall indices that span the African continent for the period 1801–1998 (Fig. 1). This date range, however, is less than one-fifth of the span of the TAST and includes only about a third of the total number of exported slaves. Thus Nicholson et al.'s (2012) indices, which include West Africa, fall short of what is needed to directly find the correlation between WA rainfall and the TAST.

Norrgård (2015) extended Nicholson et al.'s (2012) annual West African Sahel rainfall index back to 1750, but with decadal rather than annual resolution (Fig. 1). The period from 1750 to the mid-1800s constitutes less than one-third of the total time span of the TAST and less than two-thirds of the total number of

exported slaves. Although Norrgård's (2014) extended decadal rainfall index provides a substantial increase in available data for the TAST, it is not adequate for this study, which focuses on interannual variability rather than decadal variability.

To focus on interannual variability, however, poses a quandary: how do we statistically connect rainfall to the TAST given the dearth of rainfall data? To make progress, we use a reconstructed ENSO index as a proxy for WA rainfall. Thus, our first step is to establish that there is indeed a significant correlation between ENSO and WA rainfall.

2) ENSO AND WEST AFRICAN RAINFALL

ENSO is an ocean–atmosphere phenomenon that affects global weather patterns (Ropelewski and Halpert 1987; Mason and Goddard 2001). The oceanic part of ENSO is characterized by anomalous warming (El Niño) or cooling (La Niña) of sea surface temperatures in the eastern equatorial Pacific Ocean. The atmospheric part of ENSO is the Southern Oscillation, which is characterized by an east–west variation in atmospheric pressure between Tahiti and Darwin, Australia. The wind counterpart to the Southern Oscillation is the Walker circulation, which consists of two branches: a convective rising branch, in which air cools adiabatically resulting in condensation, clouds and precipitation, and a descending branch, in which air becomes warmer and drier due to adiabatic compression, which results in evaporation and the suppression of precipitation (Julian and Chervin 1978). The Pacific Walker circulation is but one of three such circulations that occur worldwide, the other two being the Atlantic and Indian Ocean Walker circulations (Cook and Vizy 2016).

Shifts in the Walker circulation over West Africa affect the region's rainfall patterns (Long et al. 2000; Joly and Voldoire 2009). Long et al. (2000), for example, analyzed 31 years of WA rainfall data and constructed empirical orthogonal functions (EOFs) of the WA 500-hPa vertical velocity field. The first EOF showed two significant circulations. A north–south Hadley circulation located east of the prime meridian and an east–west Walker circulation located over the Sahel. The rising branch of the Walker circulation, located over eastern and central Africa, corresponded with wetter conditions, while its descending branch, located throughout West Africa, corresponded with drier conditions. Joly and Voldoire (2009) used the Climate Research Unit Precipitation Climatology dataset and the Hadley Centre Sea Ice and Sea Surface Temperature dataset to construct an ENSO principal component analysis and a maximum covariance analysis to determine how WA rainfall varies with ENSO. They showed that at the onset of an El Niño event, anomalous subsidence occurred over West Africa due to an eastward shift of the Walker circulation. This subsidence favored droughts in the Sahel.

The connection between ENSO and WA rainfall also has been shown in other studies (Janicot et al. 2001; Balas et al. 2007; Barandiaran and Wang 2014; Okonkwo et al. 2014; and Okonkwo 2014). Balas et al. (2007), for example, used the International Comprehensive Ocean–Atmosphere Data Set (Worley et al. 2005) and an African rainfall dataset (Nicholson et al. 2018a,b) to obtain the seasonal variability of
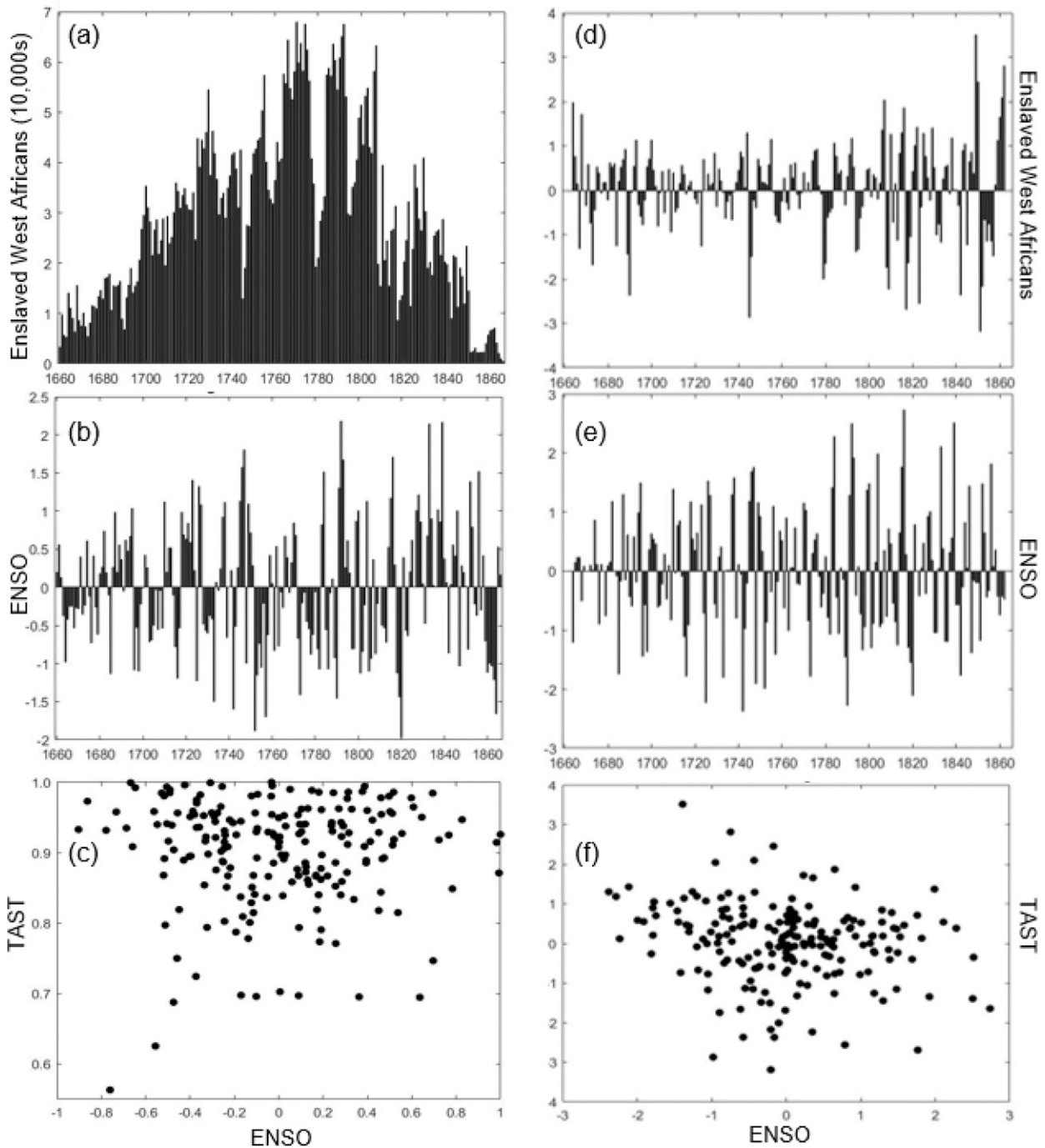
FIG. 5. (a)–(c) Raw data and (d)–(f) the detrended data for three groupings: (top) the TAST data for the period 1660–1866, (middle) an example of a reconstructed ENSO index used in this study (McGregor et al. 2010), and (bottom) a scatterplot of the relationship between ENSO and the TAST at the 2-yr lag. See the text for additional details.

the driest and wettest periods over the Sahel. They found that La Niña was linked to the wettest periods, whereas El Niño was linked to the driest periods. Barandiaran and Wang (2014) used rain gauge observations from NOAA's Precipitation over Land dataset, the National Centers for Environmental Prediction and National Corporation for Atmospheric

Research Reanalysis I atmospheric data, and the Niño-3.4 index to show that during an El Niño, the tropical easterly jet weakened, which suppressed convection over the Sahel. Okonkwo (2014) used the Global Precipitation Climatology Project, version 2, monthly rainfall anomalies from the National Oceanic and Atmospheric Administration and the

Present-day ENSO and Sahel Rainfall Regression Coefficients					
Lag	Bove et al. 1998	Rayner et al. 2003	NOAA 2020a	NOAA 2020b	Average Index
0	r = -0.2320 p = 0.0913 s = 0.1158	r = -0.3459 p = 0.0004 s = 0.0945	r = -0.3524 p = 0.0097 s = 0.1259	r = -0.0918 p = 0.6698 s = 0.2335	r = -0.2229 p = 0.2951 s = 0.4269
1	r = -0.1617 p = 0.2427 s = 0.1907	r = -0.0888 p = 0.3751 s = 0.1156	r = -0.1138 p = 0.4170 s = 0.1687	r = 0.1084 p = 0.6142 s = 0.1953	r = 0.0635 p = 0.7682 s = 0.1877
2	r = 0.2368 p = 0.0846 s = 0.1921	r = 0.0868 p = 0.3857 s = 0.1342	r = -0.0146 p = 0.9173 s = 0.2146	r = 0.2955 p = 0.1610 s = 0.2055	r = 0.3356 p = 0.1088 s = 0.2461
3	r = 0.0206 p = 0.8826 s = 0.1472	r = -0.0942 p = 0.3461 s = 0.1245	r = -0.1662 p = 0.2342 s = 0.2022	r = -0.1294 p = 0.5468 s = 0.2203	r = -0.1828 p = 0.3925 s = 0.2242

Fig. 6. Regression coefficients r, p values, and the standard errors s that relate the present-day Sahel rainfall index developed by Mitchell (2016) with the four present-day ENSO indices [Bove et al. (1998), Rayner et al. (2003), oceanic Niño index (NOAA 2020a), and multivariate ENSO index, version 2 (NOAA 2020b)] and the average index, which was obtained by averaging the data for each year from the four present-day ENSO indices. Upward or downward arrows respectively represent a positive or negative coefficient; the black arrows are significant at $p \leq 0.05$, gray arrows are significant at $p \leq 0.15$, and the white arrows are significant at $p > 0.15$.

Global Historical Climatology Network, and Niño-3.4 sea surface temperature data to conduct a wavelet analysis. Okonkwo (2014) found that El Niño events were significantly correlated with Sahel droughts.

3) PRESENT-DAY ENSO INDICES AND RAINFALL

To establish ENSO as a proxy for WA rainfall, we begin by establishing the correlation between present-day ENSO indices and a present-day Sahel rainfall index. To ensure that the correlation we find between ENSO and present-day rainfall is robust, we examine four present-day ENSO indices: 1) Bove et al. (1998); 2) Rayner et al. (2003); 3) oceanic Niño index (NOAA 2020a); and 4) multivariate ENSO index, version 2 (NOAA 2020b). We also compute an average ENSO index, which was obtained by averaging the data for each year from the four ENSO indices. For present-day Sahel rainfall, we use Mitchell's (2016) Sahel rainfall index. Mitchell (2016) used the Deutscher Wetterdienst Global Precipitation Climatology (Becker et al. 2013) to produce the Sahel rainfall index from 1901 to 2016. We used a multiple linear regression model to determine the regression coefficients between the five ENSO indices (four present-day indices and the average) and the present-day Sahel rainfall index.

Figure 6 shows the regression coefficients, p values, and standard errors obtained from the linear regression model. At the zero lag, the regression coefficients agree in sign but differ in statistical significance. Three of the five regression coefficients are significant at $p \leq 0.15$; two of five are significant at $p < 0.05$, with the strongest coefficient associated with the oceanic Niño index (NOAA 2020a). The signs of the regression coefficients are consistent with the physics-based modeling studies of Long et al. (2000) and Joly and Voldoire (2009); that is, El Niño conditions are associated with drier conditions

in the Sahel during the same year. We also computed the lag coefficients for years 4, 5, and 6, but they were much less consistent in sign and in statistical significance.

f. Selecting a reconstructed ENSO index

In the previous subsection we established, in agreement with prior studies, that ENSO is significantly associated with present-day Sahel rainfall at a zero lag. Now that we have established that ENSO can be used as a proxy for WA rainfall, our next step is to correlate ENSO with the TAST. Before doing so, however, we must first obtain a reliable ENSO reconstruction that overlaps with the TAST. By reliable we mean that an ENSO reconstruction, like the four present-day ENSO indices used in the previous section, must be significantly associated with the present-day Sahel rainfall index at a zero lag, such that El Niño is associated with drier conditions. This is our criterion for choosing an ENSO reconstruction.

ENSO reconstructions are obtained using different methods and different proxy data (Wilson et al. 2010). To ensure our results are robust, we tested seven ENSO reconstructions.[3] Of the seven, four meet our criterion: Quinn et al. (1987), Cook et al. (2008), Gergis and Fowler (2009), and McGregor et al. (2010). Quinn et al.'s (1987) El Niño–only index, which spans 1525–1987, was constructed by combining documentary and instrumental data from northern South America. Cook et al.'s (2008) ENSO index, which spans 1300–1979 (~700 years), was constructed using tree rings from Mexico and Texas. Gergis and Fowler's (2009) ENSO index,

---

[3] The seven ENSO reconstructions that we tested are Quinn et al. (1987), Cook et al. (2008), Braganza et al. (2009), Gergis and Fowler (2009), McGregor et al. (2010), Li et al. (2011), and Li et al. (2013).

Lag	Q	C	G	M	Average Index
Reconstructed ENSO and Sahel Rainfall Regression Coefficients					
0	r = −0.1924 p = 0.0958 s = 0.1065	r = −0.2654 p = 0.0093 s = 0.0994	r = −0.2820 p = 0.0071 s = 0.1204	r = −0.2633 p = 0.0327 s = 0.1204	r = −0.3802 p = 0.0016 s = 0.1488
1	r = −0.2221 p = 0.0538 s = 0.1006	r = 0.1910 p = 0.0637 s = 0.1180	r = 0.0116 p = 0.9136 s = 0.0875	r = 0.1976 p = 0.1118 s = 0.1191	r = 0.1849 p = 0.1371 s = 0.1064
2	r = 0.1530 p = 0.1871 s = 0.1217	r = −0.0370 p = 0.7221 s = 0.0924	r = −0.0413 p = 0.6990 s = 0.1059	r = −0.1313 p = 0.2935 s = 0.1043	r = −0.2694 p = 0.0287 s = 0.1224
3	r = −0.1081 p = 0.3526 s = 0.1156	r = 0.1082 p = 0.2964 s = 0.0810	r = 0.1810 p = 0.0878 s = 0.0939	r = 0.3398 p = 0.0052 s = 0.1201	r = 0.2747 p = 0.0256 s = 0.1162

FIG. 7. Regression coefficients r, p values, and the standard errors s relating the present-day Sahel rainfall index developed by Mitchell (2016) and the four ENSO reconstructions [Quinn et al. (1987) (Q), Cook et al. (2008) (C), Gergis and Fowler (2009) (G), and McGregor et al. (2010) (M)] and the average index, which was obtained by averaging the data for each year from the four reconstructed ENSO indices. See the text for further details. Upward or downward arrows respectively represent a positive or negative coefficient; the black arrows are significant at $p \leq 0.05$, gray arrows are significant at $p \leq 0.15$, and the white arrows are significant at $p > 0.15$.

which spans 1525–2002 (~500 years), was constructed using various global proxy data, including tree rings, coral sequences, and documentary records that were calibrated to the coupled ENSO index (Gergis and Fowler 2005). McGregor et al.'s (2010) ENSO index, which spans 1650–1977 (~350 years), was constructed using a principal component analysis to combine 10 ENSO proxies into a unified ENSO proxy.

Figure 7 lists the four reconstructed ENSO indices, their average, and their regression coefficients, which measure the relationship between ENSO and Sahel rainfall. Four of the five coefficients are statistically significant at $p < 0.05$; one is statistically significant at $p = 0.096$. The reconstructed ENSO indices are consistent with the present-day ENSO indices; the reconstructed and present-day indices both show that El Niño conditions are associated with drier conditions in the Sahel during the same year. This lends confidence in the ability of the reconstructed indices to yield reliable results when relating ENSO with the TAST.

3. Results and discussion

Figure 8 shows the regression coefficients, p values, and standard errors that measure the connection between the five ENSO indices and the TAST. The signs of the 0-, 1-, and 3-yr lag regression coefficients are neither consistent in sign nor statistically significant. The 2-yr lag regression coefficients, however, are consistent in sign across all of the ENSO indices: two of the five coefficients are small but significant at $p < 0.05$; four of the five coefficients are small but significant at $p < 0.15$. The 2-yr lag implies that the ENSO-induced rainfall anomaly produces a delayed response in the TAST, a response characterized by an El Niño–induced *decrease* in the number of enslaved West Africans exported out of West Africa. Such a delayed response is conceivable, since ENSO-induced drought may impart agricultural stresses that would take time to manifest in the societies involved in the TAST.

In a review of studies that examine climate and conflict, Burke et al. (2015) suggest that in linear regression models that possess multiple lags, such as ours, the lagged regression coefficients should be summed to yield a net effect. For example, as Burke et al. (2015) explain, if a lagged coefficient for one year is the same in magnitude but opposite in sign to that of another year, then the net effect would be zero. In this study, only the 2-yr lag is significant, which dominates the net effect of ENSO on the TAST.

Although anomalous rainfall is associated with agricultural stresses (Nieuwolt 1982; Lobell and Burke 2008), anomalous temperatures can also play a role (Hatfield and Prueger 2015; Bhuiyan et al. 2017). For example, warmer temperatures acting in concert with rainfall deficits could exacerbate agricultural stresses, leading to a greater influence on the TAST.

To determine whether ENSO is indeed associated with warmer temperatures in the Sahel, we correlated each of the four reconstructed ENSO indices listed in Fig. 7 with Mann et al.'s (1998) reconstructed Sahel temperature anomalies. Mann et al.'s (1998) temperature reconstruction involved combining annually resolved, multiproxy data networks, which include dendroclimatic, ice core, ice melt, and historical records. The multiproxy networks were calibrated against patterns of temperature variability in the instrumental record, from which annual mean anomalies were constructed for the reference period 1902–80 and placed on a 5° × 5° grid. Our analysis shows that, for each of the four reconstructed ENSOs, El Niño is most strongly correlated ($p < 0.000\,001$) with warmer Sahel temperatures at a zero lag. Physics-based modeling studies also show a connection between El Niño and warmer Sahel temperatures (Rayner et al. 2003; Moron et al. 2016; Oueslati et al. 2017).

		Reconstructed ENSO and TAST Regression Coefficients			
Lag	Q	C	G	M	Average Index
0	r = 0.0266 p = 0.7110 s = 0.0649 ⇑	r = -0.0101 p = 0.8884 s = 0.0698 ⇓	•	r = 0.0068 p = 0.9243 s = 0.0708 ⇑	r = 0.0180 p = 0.8027 s = 0.0711 ⇑
1	r = 0.0373 p = 0.6034 s = 0.0729 ⇑	r = -0.0652 p = 0.3637 s = 0.0560 ⇓	r = -0.0049 p = 0.9459 s = 0.0670 ⇓	r = -0.0340 p = 0.6366 s = 0.0657 ⇓	r = -0.0051 p = 0.9430 s = 0.0684 ⇓
2	r = -0.0234 p = 0.7452 s = 0.0741 ⇓	r = -0.1752 p = 0.0140 s = 0.0567 ⬇	r = -0.1266 p = 0.0771 s = 0.0737 ⬇	r = -0.1965 p = 0.0058 s = 0.0704 ⬇	r = -0.1352 p = 0.0589 s = 0.0728 ⬇
3	r = -0.0318 p = 0.6581 s = 0.0884 ⇓	r = -0.0838 p = 0.2431 s = 0.0774 ⇓	r = 0.0503 p = 0.4840 s = 0.0771 ⇑	r = -0.0337 p = 0.6393 s = 0.0949 ⇓	r = -0.0320 p = 0.6556 s = 0.0921 ⇓

FIG. 8. Fig. 8. Regression coefficients r, p values, and the standard errors s relating the TAST and each ENSO reconstruction used in this study for the period 1660–1866 [Quinn et al. (1987) (Q), Cook et al. (2008) (C), Gergis and Fowler (2009) (G), McGregor et al. (2010) (M)] and the average index, which was obtained by averaging the data for each year from the four reconstructed ENSO indices. Upward or downward arrows represent a positive or negative coefficient; the black arrows are significant at $p \leq 0.05$, gray arrows are significant at $p \leq 0.15$, and the white arrows are significant at $p > 0.15$. The black dot indicates $r < 10^{-4}$.

Moron et al. (2016), for example, used available temperature data from the Global Surface Summary of the Day and Global Historical Climate Network to show that warmer Sahel temperatures lag an El Niño event by one year. They explain their results in terms of El Niño–induced shifts in the upper and lower-tropospheric circulations over the tropics. For the upper-tropospheric circulation, anomalous diabatic heating over the central and eastern Pacific Ocean produces anomalous deep convection, which is transported eastward by equatorial Kelvin waves and westward by equatorial Rossby waves. Together these waves form a teleconnection between the El Niño warming of the Pacific Ocean and the anomalous subsidence that occurs in regions throughout the tropical atmosphere. As noted by Moron et al. (2016), the subsidence, and its attendant adiabatic warming of tropical northern Africa, particularly the Sahel, is simply a manifestation of the far-field response to El Niño. For the lower-tropospheric circulation, the trade winds weaken during El Niño, which allows for the lower layer of the atmosphere to warm. This warm layer could then be transported to the Sahel, further increasing the region's temperatures.

To summarize, our results show that during an El Niño event, which we show is associated with less rainfall and warmer temperatures over WA, slave exports decrease at a *2-yr lag*. Similar to our study, Fenske and Kala (2015) show that anomalously warm temperatures are associated with a decrease in slave exports, but, in contrast to our study, their association between temperature and the TAST is at a *zero lag*. Boxell's (2019) results, however, differ from both ours and Fenske and Kala's (2015). Specifically, Boxell (2019) shows 1) less rainfall increases slave exports at a *zero lag*, and 2) anomalously warm or anomalously cool temperatures are associated with an increase in slave exports at a *1-yr lag*. What accounts for the differences between these three studies?

To answer this question, it is instructive to first restate a key difference between this study and that of Fenske and Kala (2015). Here we use a multiple linear regression model to relate ENSO, and its proxy association with WA rainfall and temperature, with slave exports from West Africa, whereas Fenske and Kala (2015) use a regression model to relate anomalous temperatures with slave exports from specific ports throughout Africa. In a brief statement, however, Fenske and Kala (2015) note they find "no evidence that the effect of temperature differed during years with El Niño events." But it is unclear how they reached that conclusion, though they do state that it was based, in part, on Couper-Johnston (2000), who used Quinn et al.'s (1987) reconstructed El Niño index, among others. The Quinn et al. (1987) index, as we have shown earlier, has been superseded by other reconstructed ENSO indices, and, most important, we find that its relationship with the TAST is much less significant than the others. Furthermore, our statistical results, as well as the statistical and modeling results of others we cited earlier, all agree that during the warm phase of ENSO (El Niño) the temperatures over North Africa, which includes West Africa, are anomalously warm, which can be explained in terms of El Niño–induced global circulation changes.

An answer to the above question relating to the difference between our results and that of Fenske and Kala (2015) may reside in the fact that the temperature anomalies they used are a response to an amalgamation of weather and climate forcings. For instance, in addition to the ENSO modulation of rainfall and temperature over North Africa, as shown here and in other studies, the North Atlantic Oscillation (NAO) and the Atlantic multidecadal oscillation (AMO) can also affect temperature fluctuations over North Africa (Folland et al. 2009; Martin and Thorncroft 2014). Folland et al. (2009), for example, used mean sea level pressure anomalies to show that the summer NAO, which is the seasonal pressure

difference between the Icelandic low and the Azores high, is negatively correlated with Sahel rainfall and positively correlated with Sahel temperatures. Martin and Thorncroft (2014) used several observational and reanalysis datasets, including the Hadley Centre Global Sea Ice and Sea Surface Temperature dataset and the Climate Research Unit 3.1 precipitation dataset, along with the NCEP–NCAR reanalysis dataset, to show that the AMO, which is a warming or cooling of sea surface temperatures in the North Atlantic, significantly correlates with Sahel rainfall and temperature. Specifically, during the warm phase of the AMO, Sahel rainfall is enhanced while temperatures are cooler.

We also note that Fenske and Kala (2015) use a single temperature reconstruction for their analysis, one based on Mann et al. (1998). It is not clear to what extent their results are a consequence of the reconstruction they used. For example, the Mann et al. (1998) reconstruction was developed using a multiproxy approach, which depends on the spatial and temporal scale of the available data and on how each proxy is weighted. As shown in Jones et al. (1998), for example, the strength of proxies can be ranked from strongest to weakest as follows: instrumental records, historical records, tree rings, ice cores, and corals. Thus, like the ENSO reconstructions that we examined, different temperature reconstructions may yield different results. Indeed, Wang et al. (2020) have shown that significant differences may arise between different reconstructed temperature indices. For example, out of 18 reconstructed temperature indices and 6 model simulations, they found that the covariance among them became increasingly different as they moved farther back in time. Reconstructed temperature indices also are constructed using different proxy data that vary based on temporal and spatial scales (Mann 2002). For example, coral reefs describe tropical environments, but lack multicentury records (Mann 2002).

Boxell (2019) shows that the response of the TAST to temperature is nonuniform and most significant at a 1-yr lag; the response is described by a parabolic-like curve, with the apex separating anomalously cool temperatures from anomalously warm temperatures. The curve shows that the number of slave exports increases monotonically as the anomalously cool or warm temperatures increase. Although this temperature–TAST relationship is strikingly different from Fenske and Kala's (2015), Boxell (2019) makes clear that the difference is likely due to the different time spans used in the two studies: Fenske and Kala (2015) analyzed the period 1730–1866, a span of 117 years, whereas Boxell (2019) analyzed the period 1801–66, a span of 66 years. Boxell's (2019) 66-yr span is also far shorter than what we have examined.

Boxell's (2019) shorter analysis period was based on the limited availability of African rainfall data, which he also correlated with the TAST. Boxell (2019) used Nicholson's (2001) reconstructed African rainfall dataset, which spans 1801–1900. Boxell (2019) found that during drier conditions the number of slave exports increased at a 1-yr lag. It is unclear, however, whether Boxell's (2019) results would change, and perhaps be more aligned with ours, if Nicholson et al.'s (2012) updated African rainfall dataset were used.

The differences between our results and those of Fenske and Kala (2015) and Boxell (2019) may also be due to differences in the geographical focus and time periods between the studies. For example, Fenske and Kala (2015) and Boxell (2019) both study the export of enslaved Africans from regions throughout Africa, but from 1730 to 1866 and 1801 to 1866, respectively. In contrast, this study focuses on the export of enslaved Africans from West Africa from 1660 to 1866. Moreover, after the British enacted the Slave Trade Act in 1807, most of the slaves were exported from central Africa (Boxell 2019), a region that is not considered in this study.

4. Concluding remarks

The transatlantic slave trade was driven by economic and political forces, subject to the vagaries of the weather; it spanned two hemispheres and four continents and lasted more than 400 years. Here we presented statistical evidence that supports our original hypothesis: El Niño–Southern Oscillation, and its proxy association with West African rainfall and temperature, modulated the number of enslaved Africans that were transported from West Africa to the Americas. To test our hypothesis, we used the Slave Voyages dataset, and to ensure that our results are robust, we used four reconstructed ENSO datasets and a multiple linear regression model to determine the statistical relationship between ENSO and the TAST.

The statistical analysis shows a small but statistically significant association between ENSO and the TAST at a 2-yr lag. At this lag, El Niño is associated with a *decrease* in the number of enslaved Africans transported from West Africa to the Americas.

Our analysis centered on the proxy association between ENSO and West African rainfall and temperature, and how that association affected the TAST. Our focus on rainfall was based on a key factor: rainfall outweighs temperature when it comes to agricultural production (Nieuwolt 1982; Lobell and Burke 2008), which historians have deemed to be a primary determinant in affecting the migration and enslavement of African people during the TAST. Although rainfall tends to outweigh temperature when it comes to agricultural production, temperature may still play a role. For this reason, we also examined the proxy association between ENSO and temperature. In agreement with other studies (see section 3), we show that in the Sahel, El Niño (drier conditions) is associated with anomalously warm temperatures. The warmer temperatures and rainfall deficits would act in concert to exacerbate the dry conditions, conceivably leading to a flash drought, a phenomenon associated with the rapid onset of drier conditions (Mo and Lettenmaier 2015, 2016).

Flash droughts are of two types: heat-wave flash droughts, which increase evapotranspiration and decrease soil moisture; and precipitation-deficit flash droughts, which decrease soil moisture, causing, in turn, increases in temperature by limiting evaporative cooling (Koster et al. 2009). Flash droughts occur worldwide. Mo and Lettenmaier (2016), for example, showed that flash droughts affected United States' agriculture
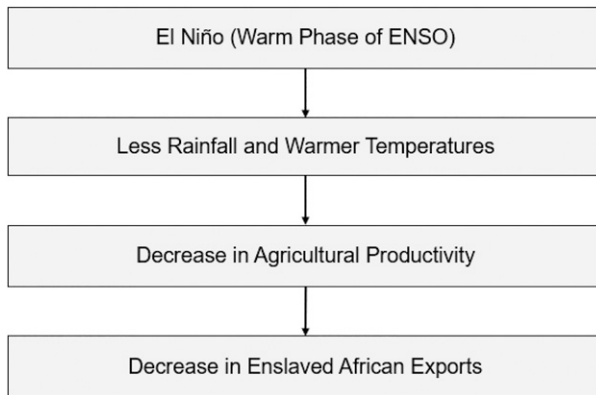
FIG. 9. The 2-yr-lag scenario linking El Niño and the TAST in West Africa. El Niño–induced drier and warmer conditions, which may lead to flash droughts, reduce agricultural production. The reduced agricultural production would cause a delayed response in the TAST, one that would yield a decrease in the number of enslaved West Africans exported to the Americas. See the text for additional details.

in the 1980s. Yuan et al. (2018) showed that flash droughts have increased in occurrence in South Africa. Although there has yet to be a comprehensive study of flash droughts over West Africa, it is plausible that they can occur there. If so, the flash droughts would have caused agricultural stresses, which would manifest in changes in the number of enslaved Africans exported to the Americas. This scenario, which links drier conditions (flash droughts) with the TAST, is illustrated in Fig. 9.

ENSO is one of several synoptic to planetary-scale circulation features that are connected to West African rainfall. Other features include the African easterly jet–African easterly wave (AEJ-AEW) system (Thorncroft and Blackburn 1999; Okonkwo et al. 2014; Bercos-Hickey et al. 2020), the NAO (Folland et al. 2009; Polo et al. 2011; Okonkwo 2014), and the AMO (Zhang and Delworth 2006; Ting et al. 2011; Okonkwo 2014). Bercos-Hickey et al. (2020), for example, used the Weather Research and Forecasting Model to examine the connection between West African rainfall and the AEJ, a current of strong easterly winds in the lower troposphere that is centered at ~15°N, that is, between the Sahara Desert to the north and the Guinea coast to the south. They showed that variations in the strength, location, and spatial orientation of the AEJ are tied to variations in both rainfall and Saharan dust aerosols. Folland et al. (2009) showed that the summer NAO was negatively correlated with Sahel rainfall and positively correlated with Sahel temperatures. Okonkwo (2014) used a wavelet analysis to show that the cooler phase of AMO was associated with Sahel droughts. Adding to the complexity of the problem is the fact that the AEJ-AEW system, NAO, AMO, and ENSO could conceivably act in isolation or in combination to affect the TAST.

From an economics perspective, the TAST was driven by supply and demand. The Africans enslaved in North Africa provided the manpower needed to meet the demand for commodities such as sugar and tobacco in the Americas. Here we have focused on the supply side of the TAST, in which ENSO and its proxy association with temperature and rainfall over West Africa was shown to be statistically associated with changes in the number of enslaved Africans transported to the Americas. ENSO, however, also affects temperature and rainfall during certain times and over certain regions of the Americas (Kiladis and Diaz 1989; Diaz and Markgraf 1992). Thus, it is conceivable that ENSO could modulate both the supply and demand sides of the TAST. For example, on the basis of the El Niño and La Niña phases of the Southern Oscillation (SO), Kiladis and Diaz (1989) produced composite temperature and precipitation anomalies for the period spanning 1877–1988 for several hundred stations across the globe. Their study shows strong intraseasonal, interannual and regional variability in the temperature and precipitation response to the SO in West Africa and the Americas. Consequently, determining whether the ENSO-modulated supply and demand sides of the TAST operated in concert or in opposition is a daunting task, one fraught with significant challenges. Among the challenges is timing, which includes the differences between the onset of ENSO, the responses in temperature and precipitation in West Africa and the Americas, and the TAST itself. And there is the issue of ENSO-induced stresses on the political and economic structures of the societies themselves, which were manifestly different between West Africa and the Americas. Despite these challenges and others, addressing how ENSO affected the supply and demand sides of the TAST is an important problem, one that should be addressed in the future.

In addition to the limitations associated with neglecting other climate forcings and the supply and demand sides of the TAST, there are other factors that could affect our results. These include measurement errors associated with the instrumental and proxy data used in the historical reconstructions of the ENSO indices. In addition, our analysis relied on time series data that did not account for geographic variations. Such variations are difficult to assess, however, since current ENSO reconstructions are not detailed enough to provide reliable subsynoptic-scale information on rainfall and temperature over West Africa.

We close with the West African word—sankofa, which roughly translates to the past informs the future (Quarcoo 1972). Sankofa is an apt embodiment of this paper, which adds to the many other historical and present-day studies that have shown a connection between weather and climate and their effects on society. The NAO, for example, and its association with drier conditions in Europe, has been suggested as a contributing factor to the fall of the Roman Empire (Drake 2017). Studies have shown that the severe droughts of the twelfth and thirteenth centuries in the southwestern United States were the impetus for the migration of the Anasazi Indians from their ancestral homeland in Mesa Verde to more hospitable locales (Van West and Dean 2000; Benson et al. 2007). More recently, droughts have been identified as a contributing factor to the Syrian war. From 2006 to 2011, Syria experienced one of their worst droughts on record (Kelley et al. 2015; Cook et al. 2016). Coupled with ineffective policies for water management, agriculture failures, and an increasing

population, the drought forced more than one million farmers and rural citizens to migrate into urban areas within one year (Gleick 2014; Richani 2016). The United Nations Office for the Coordination of Humanitarian Affairs's (2017) report estimates that the Syrian war caused more than 11 million Syrians to be displaced within and outside of Syria.

Lessons learned from the effects of weather and climate on the TAST reverberate today: extreme weather and climate change will continue to catalyze and amplify human conflict and migrations.

REFERENCES

American Meteorological Society, 2020: Drought. *Glossary of Meteorology*, http://glossary.ametsoc.org/wiki/Drought.

Amrhein, V., S. Greenland, and B. McShane, 2019a: Scientists rise up against statistical significance. *Nature*, **567**, 305–307, https://doi.org/10.1038/d41586-019-00857-9.

——, D. Trafimow, and S. Greenland, 2019b: Inferential statistics as descriptive statistics: There is no replication crisis if we don't expect replication. *Amer. Stat.*, **73**, 262–270, https://doi.org/10.1080/00031305.2018.1543137.

Anderson, F., 2000: *The Crucible of War: The Seven Years' War and the Fate of Empire in British North America, 1754–1766.* Knopf, 862 pp.

Anstey, R., 1972: A re-interpretation of the abolition of the British slave trade, 1806–1807. *Engl. Hist. Rev.*, **LXXXVII**, 304–332, https://doi.org/10.1093/ehr/LXXXVII.CCCXLIII.304.

Bailey, R., 1994: The other side of slavery: Black labor, cotton, and textile industrialization in Great Britain and the United States. *J. Agric. Hist.*, **68**, 35–50.

Balas, N., S. E. Nicholson, and D. Klotter, 2007: The relationship of rainfall variability in West Central Africa to sea-surface temperature fluctuations. *Int. J. Climatol.*, **27**, 1335–1349, https://doi.org/10.1002/joc.1456.

Barandiaran, D., and S.-Y. Wang, 2014: The missing teleconnection between the North Atlantic and the Sahel precipitation in CFSv2. *Atmos. Sci. Lett.*, **15**, 21–28, https://doi.org/10.1002/asl2.457.

Becker, A., P. Finger, A. Meyer-Christoffer, B. Rudolf, K. Schamm, U. Schneider, and M. Ziese, 2013: A description of the global land-surface precipitation data products of the Global Precipitation Climatology Centre with sample applications including centennial (trend) analysis from 1901–present. *Earth Syst. Sci. Data*, **5**, 71–99, https://doi.org/10.5194/essd-5-71-2013.

Benson, L., K. Petersen, and J. Stein, 2007: Anasazi (Pre-Columbian Native-American) migrations during the middle-12th and late-13th centuries—Were they drought induced? *Climatic Change*, **83**, 187–213, https://doi.org/10.1007/s10584-006-9065-y.

Bercos-Hickey, E., T. R. Nathan, and S. H. Chen, 2020: On the relationship between African easterly jet, Saharan mineral dust aerosols, and West African precipitation. *J. Climate*, **33**, 3533–3546, https://doi.org/10.1175/JCLI-D-18-0661.1.

Bethell, L., 1966: The mixed commissions for the suppression of the transatlantic slave trade in the nineteenth century. *J. Afr. Hist.*, **7**, 79–93, https://doi.org/10.1017/S0021853700006095.

Bhuiyan, C., A. K. Saha, N. Bandyopadhyay, and F. N. Kogan, 2017: Analyzing the impact of thermal stress on vegetation health and agricultural drought—A case study from Gujarat, India. *GISci. Remote Sens.*, **54**, 678–699, https://doi.org/10.1080/15481603.2017.1309737.

Blackburn, R., 1988: *The Overthrow of Colonial Slavery, 1776–1848.* Verso, 560 pp.

Bove, M. C., J. B. Elsner, C. W. Landsea, X. Niu, and J. J. O'Brien, 1998: Effect of El Niño on U.S. landfalling hurricanes, revisited. *Bull. Amer. Meteor. Soc.*, **79**, 2477–2482, https://doi.org/10.1175/1520-0477(1998)079<2477:EOENOO>2.0.CO;2.

Boxell, L., 2019: Droughts, conflict, and the African slave trade. *J. Comp. Econ.*, **47**, 774–791, https://doi.org/10.1016/j.jce.2019.06.002.

Braganza, K., J. L. Gergis, S. B. Power, J. S. Risbey, and A. M. Fowler, 2009: A multiproxy index of the El Niño–Southern Oscillation, A.D. 1525–1982. *J. Geophys. Res.*, **114**, D05106, https://doi.org/10.1029/2008JD010896.

Burke, M., S. M. Hsiang, and E. Miguel, 2015: Climate and conflict. *Annu. Rev. Econ.*, **7**, 577–617, https://doi.org/10.1146/annurev-economics-080614-115430.

Chen, S.-H., Y.-C. Liu, T. R. Nathan, C. Davis, R. Torn, N. Sowa, C.-T. Cheng, and J.-P. Chen, 2015: Modeling the effects of dust-radiative forcing on the movement of Hurricane Helene (2006). *Quart. J. Roy. Meteor. Soc.*, **141**, 2563–2570, https://doi.org/10.1002/qj.2542.

Cook, B. I., K. J. Anchukaitis, R. Touchan, D. M. Meko, and E. R. Cook, 2016: Spatiotemporal drought variability in the Mediterranean over the last 900 years. *J. Geophys. Res. Atmos.*, **121**, 2060–2074, https://doi.org/10.1002/2015JD023929.

Cook, E. R., R. D. D'Arrigo, and K. J. Anchukaitis, 2008: 700 year tree-ring ENSO index reconstructions. NOAA/National Centers for Environmental Information, accessed 2 January 2017, https://www.ncei.noaa.gov/access/paleo-search/study/8704.

Cook, K. H., and E. Vizy, 2016: The Congo basin Walker circulation: Dynamics and connections to precipitation. *Climate Dyn.*, **47**, 697–717, https://doi.org/10.1007/s00382-015-2864-y.

Couper-Johnston, R., 2000: *El Niño: The Weather Phenomenon the Changed the World.* Hodder and Stoughton, 354 pp.

Craton, M., 1974: *Sinews of Empire: A Short History of British Slavery.* Anchor Press, 413 pp.

Curtin, P. D., 1972: *The Atlantic Slave Trade: A Census.* University of Wisconsin Press, 357 pp.

Dias, J. R., 1981: Famine and disease in the history of Angola c. 1830–1930. *J. Afr. Hist.*, **22**, 349–378, https://doi.org/10.1017/S0021853700019575.

Diaz, H. F., and V. Markgraf, 1992: *El Niño: Historical and Paleoclimatic Aspects of the Southern Oscillation.* Cambridge University Press, 475 pp.

Drake, B. L., 2017: Changes in North Atlantic Oscillation drove population migrations and the collapse of the western Roman Empire. *Sci. Rep.* **7**, 1227, https://doi.org/10.1038/s41598-017-01289-z.

Du Bois, W. E. B., 1896: *The Suppression of the African Slave Trade to the United States of America, 1638–1870.* Longman, 365 pp.

Eltis, D., 1987a: The nineteenth-century transatlantic slave trade: An annual time series of imports into the Americas broken down by region. *Hisp. Amer. Hist. Rev.*, **67**, 109–138, https://doi.org/10.1215/00182168-67.1.109.

——, 1987b: *Economic Growth and the Ending of the Transatlantic Slave Trade*. Oxford University Press, 434 pp.

——, F. D. Lewis, and L. Richardson, 2005: Slave prices, the African slave trade, and productivity in the Caribbean. *Econ. Hist. Rev.*, **58**, 673–700, https://doi.org/10.1111/j.1468-0289.2005.00318.x.

——, and Coauthors, 2009: Voyages: The Trans-Atlantic Slave Trade database. Slave Voyages Consortium, accessed 10 October 2014, http://www.slavevoyages.org.

Fenske, J., and N. Kala, 2015: Climate and the slave trade. *J. Dev. Econ.*, **112**, 19–32, https://doi.org/10.1016/j.jdeveco.2014.10.001.

Folland, C. K., J. Knight, H. W. Linderholm, D. Fereday, S. Ineson, and J. W. Hurrell, 2009: The summer North Atlantic Oscillation: Past, present, and future. *J. Climate*, **22**, 1082–1103, https://doi.org/10.1175/2008JCLI2459.1.

Gergis, J. L., and A. M. Fowler, 2005: Classification of synchronous oceanic and atmospheric El Niño-Southern Oscillation (ENSO) events for paleoclimate reconstruction. *Int. J. Climatol.*, **25**, 1541–1565, https://doi.org/10.1002/joc.1202.

——, and ——, 2009: A history of ENSO events since A.D. 1525: Implications for future climate change. *Climatic Change*, **92**, 343–387, https://doi.org/10.1007/s10584-008-9476-z.

Gleick, P. H., 2014: Water, drought, climate change, and conflict in Syria. *Wea. Climate Soc.*, **6**, 331–340, https://doi.org/10.1175/WCAS-D-13-00059.1.

Hatfield, J. L., and J. H. Prueger, 2015: Temperature extremes: Effect on plant growth and development. *Wea. Climate Extremes*, **10**, 4–10, https://doi.org/10.1016/j.wace.2015.08.001.

Janicot, S., S. Trzaska, and I. Poccard, 2001: Summer Sahel-ENSO teleconnection and decadal time scale SST variations. *Climate Dyn.*, **18**, 303–320, https://doi.org/10.1007/s003820100172.

Joly, M., and A. Voldoire, 2009: Influence of ENSO on the West African monsoon: Temporal aspects and atmospheric processes. *J. Climate*, **22**, 3193–3210, https://doi.org/10.1175/2008JCLI2450.1.

Jones, P. D., K. R. Briffa, T. P. Barnett, and S. F. B. Tett, 1998: High-resolution palaeoclimatic records for the last millennium: Interpretation, integration and comparison with general circulation model control-run temperatures. *Holocene*, **8**, 455–471, https://doi.org/10.1191/095968398667194956.

Julian, P. R., and R. M. Chervin, 1978: A study of the Southern Oscillation and Walker circulation phenomena. *Mon. Wea. Rev.*, **106**, 1433–1451, https://doi.org/10.1175/1520-0493(1978)106<1433:ASOTSO>2.0.CO;2.

Kelley, C. P., S. Mohtadi, M. A. Cane, R. Seager, and Y. Kushnir, 2015: Climate change in the Fertile Crescent and implications of the recent Syrian drought. *Proc. Natl. Acad. Sci. USA*, **112**, 3241–3246, https://doi.org/10.1073/pnas.1421533112.

Kiladis, G. N., and H. F. Diaz, 1989: Global climate anomalies associated with extremes in the Southern Oscillation. *J. Climate*, **2**, 1069–1090, https://doi.org/10.1175/1520-0442(1989)002<1069:GCAAWE>2.0.CO;2.

Koster, R. D., S. D. Schubert, and M. J. Suarez, 2009: Analyzing the concurrence of meteorological droughts and WA rainfall periods, with implications for the determination of evaporative regime. *Bull. Amer. Meteor. Soc.*, **22**, 333–3341, https://doi.org/10.1175/2008JCLI2718.1.

Li, J., S.-P. Xie, E. R. Cook, G. Huang, R. D'Arrigo, F. Liu, J. Ma, and X.-T. Zheng, 2011: Interdecadal modulation of El Niño amplitude during the past millennium. *Nat. Climate Change*, **1**, 114–118, https://doi.org/10.1038/nclimate1086.

——, and Coauthors, 2013: El Niño modulations over the past seven centuries. *Nat. Climate Change*, **3**, 822–826, https://doi.org/10.1038/nclimate1936.

Lobell, D. B., and M. B. Burke, 2008: Why are agricultural impacts of climate change so uncertain? The importance of temperature relative to precipitation. *Environ. Res. Lett.*, **3**, 034007, https://doi.org/10.1088/1748-9326/3/3/034007.

Long, M., D. Entekhabi, and S. E. Nicholson, 2000: Interannual variability in rainfall, water vapor flux, and vertical motion over West Africa. *J. Climate*, **13**, 3827–3841, https://doi.org/10.1175/1520-0442(2000)013<3827:IVIRWV>2.0.CO;2.

Lovejoy, P. E., 2012: *Transformations in Slavery: A History of Slavery in Africa.* 3rd ed. Cambridge University Press, 381 pp.

——, and S. Baier, 1975: The desert-side economy of the central Sudan. *Int. J. Afr. Hist. Stud.*, **8**, 551–581, https://doi.org/10.2307/216696.

Mann, M. E., 2002: The value of multiple proxies. *Science*, **297**, 1481–1482, https://doi.org/10.1126/science.1074318.

——, R. Bradley, and M. Hughes, 1998: Global-scale temperature patterns and climate forcing over the past six centuries. *Nature*, **392**, 779–787, https://doi.org/10.1038/33859.

Martin, E. R., and C. D. Thorncroft, 2014: The impact of the AMO on the West African monsoon annual cycle. *Quart. J. Roy. Meteor. Soc.*, **140**, 31–46, https://doi.org/10.1002/qj.2107.

Mason, S. J., and L. Goddard, 2001: Probabilistic precipitation anomalies associated with ENSO. *Bull. Amer. Meteor. Soc.*, **82**, 619–638, https://doi.org/10.1175/1520-0477(2001)082<0619:PPAAWE>2.3.CO;2.

M'baye, B., 2006: The economic, political, and social impact of the Atlantic slave trade on Africa. *Eur. Legacy*, **11**, 607–622, https://doi.org/10.1080/10848770600918091.

McGregor, S., A. Timmermann, and O. Timm, 2010: A unified proxy for ENSO and PDO variability since 1650. *Climate Past*, **6**, 1–17, https://doi.org/10.5194/cp-6-1-2010.

McShane, B. B., D. Gal, A. Gelman, C. Robert, and J. L. Tackett, 2019: Abandon statistical significance. *Amer. Stat.*, **73**, 235–245, https://doi.org/10.1080/00031305.2018.1527253.

Miller, J. C., 1982: The significance of drought, disease, and famine in the agriculturally marginal zones of West-Central Africa. *J. Afr. Hist.*, **23**, 17–61, https://doi.org/10.1017/S0021853700020235.

Mintz, S. W., 1986: *Sweetness and Power: The Place of Sugar in Modern History.* Penguin Books, 274 pp.

Mitchell, T. P., 2016: Sahel precipitation index. Accessed 12 November 2016, http://research.jisao.washington.edu/data/sahel/.

Mo, K. C., and D. P. Lettenmaier, 2015: Heat wave flash droughts in decline. *Geophys. Res. Lett.*, **42**, 2823–2829, https://doi.org/10.1002/2015GL064018.

——, and ——, 2016: Precipitation deficit flash droughts over the United States. *J. Hydrometeor.*, **17**, 1169–1184, https://doi.org/10.1175/JHM-D-15-0158.1.

Moron, V., B. Oueslati, B. Pohl, S. Rome, and S. Janicot, 2016: Trends of mean temperatures and warm extremes in northern tropical Africa (1961–2014) from observed and PPCA-reconstructed time series. *J. Geophys. Res. Atmos.*, **121**, 5298–5319, https://doi.org/10.1002/2015JD024303.

Mulcahy, M., 2004: Weathering the storms: Hurricanes and risk in the British Greater Caribbean. *Bus. Hist. Rev.*, **78**, 635–663, https://doi.org/10.2307/25096952.

NCDC, 1998: The Maury Collection: Global Ship Observations, 1792–1910. NCDC, CD-ROM, version 1.0.

NCEI, 2020: Definition of drought. NOAA, https://www.ncdc.noaa.gov/monitoring-references/dyk/drought-definition.

Needell, J., 2001: The abolition of the Brazilian slave trade in 1850: Historiography, slave agency and statesmanship. *J. Lat. Amer. Stud.*, **33**, 681–711, https://doi.org/10.1017/S0022216X01006204.

Newey, W. K., and K. D. West, 1987: A simple, positive semi-definite, heteroskedasticity and autocorrelation consistent covariance matrix. *Econometrica*, **55**, 703–708, https://doi.org/10.2307/1913610.

Nicholson, S. E., 2001: Climatic and environmental change in Africa during the last two centuries. *Climate Res.*, **17**, 123–144, https://doi.org/10.3354/cr017123.

——, A. K. Dezfuli, and D. Klotter, 2012: A two-century precipitation dataset for the continent of Africa. *Bull. Amer. Meteor. Soc.*, **93**, 1219–1231, https://doi.org/10.1175/BAMS-D-11-00212.1.

——, C. Funk, and C. A. Fink, 2018a: Rainfall over the African continent from the 19th through the 21st century. *Global Planet. Change*, **165**, 114–127, https://doi.org/10.1016/j.gloplacha.2017.12.014.

——, D. Klotter, A. K. Dezfuli, and L. Zhou, 2018b: New rainfall datasets for the Congo basin and surrounding regions. *J. Hydrometeor.*, **19**, 1379–1396, https://doi.org/10.1175/JHM-D-18-0015.1.

Nieuwolt, S., 1982: Tropical rainfall variability: The agroclimatic impact. *Agric. Ecosyst. Environ.*, **7**, 135–148, https://doi.org/10.1016/0304-1131(82)90003-0.

NOAA, 2020a: Oceanic Niño index. Accessed 1 June 2020, https://origin.cpc.ncep.noaa.gov/products/analysis_monitoring/ensostuff/ONI_v5.php.

——, 2020b: Multivariate ENSO index version 2. Accessed 1 June 2020, https://www.psl.noaa.gov/enso/mei/.

Norrgård, S., 2015: Practicing historical climatology in West Africa: A climatic periodisation 1750–1800. *Climatic Change*, **129**, 131–143, https://doi.org/10.1007/s10584-014-1307-9.

Okonkwo, C., 2014: An advanced review of the relationship between Sahel precipitation and climate indices: A wavelet approach. *Int. J. Atmos. Sci*, **2014**, 759067, https://doi.org/10.1155/2014/759067.

——, B. Demoz, and S. Tesfai, 2014: Characterization of West African jet streams and their association to ENSO events and rainfall in the ERA-Interim 1979–2011. *Adv. Meteor.*, **2014**, 405617, https://doi.org/10.1155/2014/405617.

Oueslati, B., P. Benjamin, M. Vincent, R. Sandra, and J. Serge, 2017: Characterization of heat waves in the Sahel and associates physical mechanisms. *J. Climate*, **30**, 3095–3115, https://doi.org/10.1175/JCLI-D-16-0432.1.

Polo, I., A. Ullmann, P. Roucou, and B. Fontaine, 2011: Weather regimes in the Euro-Atlantic and Mediterranean sector, and relationship with West African rainfall over the 1989–2008 period from a self-organizing maps approach. *J. Climate*, **24**, 3423–3432, https://doi.org/10.1175/2011JCLI3622.1.

Quarcoo, A. K., 1972: *The Language of Adinkra Symbols.* Sebewie Ventures, 60 pp.

Quinn, W. H., V. T. Neal, and S. E. Antunez De Mayolo, 1987: El Niño occurrences over the past four and a half centuries. *J. Geophys. Res.*, **92**, 14 449–14 461, https://doi.org/10.1029/JC092iC13p14449.

Rayner, N. A., D. E. Parker, E. B. Horton, C. K. Folland, L. V. Alexander, D. P. Rowell, E. C. Kent, and A. Kaplan, 2003: Global analyses of sea surface temperature, sea ice, and night marine air temperature since the late nineteenth century. *J. Geophys. Res.*, **108**, 4407, https://doi.org/10.1029/2002JD002670.

Rediker, M., 2007: *The Slave Ship: A Human History*. Viking Penguin, 434 pp.

Richani, N., 2016: The political economy and complex interdependency of the war system in Syria. *Civ. Wars*, **18**, 45–68, https://doi.org/10.1080/13698249.2016.1144495.

Ropelewski, C. F., and M. S. Halpert, 1987: Global and regional precipitation patterns associated with the El Niño/Southern Oscillation. *Mon. Wea. Rev.*, **115**, 1606–1626, https://doi.org/10.1175/1520-0493(1987)115<1606:GARSPP>2.0.CO;2.

Sheridan, R. B., 1976: The crisis of slave subsistence in the British West Indies during and after the American Revolution. *William Mary Quart.*, **33**, 615–641, https://doi.org/10.2307/1921718.

Thomas, H., 1997: *The Slave Trade, 1440–1870*. Simon and Schuster, 909 pp.

Thorncroft, C. D., and M. Blackburn, 1999: Maintenance of the African easterly jet. *Quart. J. Roy. Meteor. Soc.*, **125**, 763–786, https://doi.org/10.1002/qj.49712555502.

Ting, M., K. Yochanan, R. Seager, and C. Li, 2011: Robust features of Atlantic multi-decadal variability and its climate impacts. *Geophys. Res. Lett.*, **38**, L17705, https://doi.org/10.1029/2011GL048712.

United Nations Office for the Coordination of Humanitarian Affairs, 2017: Humanitarian Needs Overview: Syrian Arab Republic. United Nations Doc., 76 pp., https://www.humanitarianresponse.info/sites/www.humanitarianresponse.info/files/documents/files/2018_syr_hno_english_3.pdf.

Van West, C. R., and J. S. Dean, 2000: Environmental characteristics of the A.D. 900–1300 period in the central Mesa Verde region. *KIVA J. Southwest. Anthropol. Hist.*, **66**, 19–44, https://doi.org/10.1080/00231940.2000.11758420.

Wang, J., B. Yang, J. Zheng, X. Zhang, Z. Wang, M. Fang, F. Shi, and J. Liu, 2020: Evaluation of multidecadal and longer-term temperature changes since 850 CE based on Northern Hemisphere proxy-based reconstructions and model simulations. *Sci. China Earth Sci.*, **63**, 1126–1143, https://doi.org/10.1007/s11430-019-9607-x.

Wasserstein, R. L., A. L. Schirm, and N. A. Lazar, 2019: Moving to a world beyond "$p < 0.05$." *Amer. Stat.*, **73** (Suppl. 1), 1–19, https://doi.org/10.1080/00031305.2019.1583913.

Wilks, D. S., 2006: *Statistical Methods in the Atmospheric Sciences.* Elsevier, 630 pp.

Wilson, R., E. Cook, R. D'Arrigo, N. Riedwyl, M. N. Evans, A. Tudhope, and R. Allan, 2010: Reconstructing ENSO: The influence of method, proxy data, climate forcing and teleconnections. *J. Quat. Sci.*, **25**, 62–78, https://doi.org/10.1002/jqs.1297.

Worley, S. J., S. D. Woodruff, R. W. Reynolds, S. J. Lubker, and N. Lott, 2005: ICOADS release 2.1 data and products. *Int. J. Climatol.*, **25**, 823–842, https://doi.org/10.1002/joc.1166.

Yuan, X., L. Wang, and E. F. Wood, 2018: Anthropogenic intensification of southern African flash droughts as exemplified by the 2015/16 season [in "Explaining Extreme Events of 2016 from a Climate Perspective"]. *Bull. Amer. Meteor. Soc.*, **99** (1), S86–S90, https://doi.org/10.1175/BAMS-D-17-0077.1.

Zhang, R., and T. L. Delworth, 2006: Impact of Atlantic multidecadal oscillations on India/Sahel rainfall and Atlantic hurricanes. *Geophys. Res. Lett.*, **33**, L17712, https://doi.org/10.1029/2006GL026267.